Solid State Science and Technology, Vol. 24, No 1 (2016) 198-209
ISSN 0128-7389 | *http://journal.masshp.net*

EFFECT OF SINTERING TEMPERATURE ON STRUCTURE, MICROSTRUCTURE AND MAGNETIC PROPERTIES OF $La_{0.67}Ca_{0.33}MnO_3$ SYNTHESIZED VIA SOL-GEL METHOD

W. N. W. Wan Jusoh[1], K. P. Lim[1], M. M. Awang Kechik[1], S. A. Halim[1], S. W. Ng[1] and H. S. Woon[2]

[1]*Superconductor Laboratory, Department of Physics, Faculty of Science, Universiti Putra Malaysia, 43400 Serdang, Selangor.*

[2]*Department of Mechanical Engineering, College of Engineering, Universiti Tenaga Malaysia, Jalan IKRAM-UNITEN, 43000, Kajang, Selangor*

Corresponding author: limkp@upm.edu.my

ABSTRACT

A systematic investigation of high purity powder of managenese perovskite polycrystalline $La_{0.67}Ca_{0.33}MnO_3$ (LCMO) has been undertaken in view to understanding the effect of varying temperature ranging between 600ºC and 1200ºC on structure, microstructure and magnetic properties using Sol-Gel method. The Thermogravimetric analysis (TGA) shows at 600°C – 700°C, decomposition of the carbonates are completed and crystalline into the perovskite phase. X-ray diffraction (XRD) patterns show that parent compound of $La_{0.67}Ca_{0.33}MnO_3$ was in single phase without any detectable impurity and give orthorhombic structure with space group *Pbnm* (62). Rietveld refinement analysis showed no significant change on lattice parameter. Field emission scanning electron microscopy (FESEM) shows that the lowest particle size is 29.29 nm sintered at 600ºC and grain size growth to 722 nm with increment of sintering temperature to 1200ºC. The particle size as well as crystallite size shows a strong dependence on the sintering temperature. As the grain size growth from 29 nm to 722 nm, the coercivity value increase to the maximum at 24.7 G and the value drop as the grain size further increase. The variation of the coercivity is believed to be due to the evolution from single domain to multi domain condition. The highest coercivity at two domain or pseudo-single domain condition is due to the effect of magnetostatic and exchange energy.

Keywords: Sol-gel; structural; grain boundaries; magnetic materials; perovskite manganites;

INTRODUCTION

Perovskite manganites with general formula $La_{1-x}A_xMnO_3$ where A is a divalent alkaline earth cation (e.g Ca, Ba, Sr) has attracted extensive attention in the last few decades due to its special physical properties and potential applications in magnetoresistive devices [1]. It is proved that Jahn-Teller effect and double exchange

(DE) mechanism that attributed to paramagnetic insulator state or antiferromagnetic insulating state and ferromagnetic metallic state is mostly conceived to be the relation of the rich physical properties in colossol magnetoresitance (CMR) materials. The effect of grain size on magnetic behaviors of different types of manganites had been studied by many researchers [2,3]. Goutam *et al.,* (2006) [4] studied the effect of sintering temperature (T_s) from 600°C to 1000°C in nanophase $La_{0.7}Ca_{0.3}MnO_3$ manganites synthesized through polymeric precursor route and he observed that as T_s increased, both crystallite size and the particle size were increased due to the congregation effect. The magnetic behavior change and lattice parameter decrease in systematic way as sintering temperature decrease, while microstructure reveals that particle also decrease from ~200 nm (1000°C) to ~50 nm (700°C). The effect of grain size reduction on the magnetization curve is associated to the magnetic behavior between the surface and the core for the granular system which had been proposed by Huang *et al* (2003) [5]. Several techniques are available to prepare LCMO powders such as solid state reaction [6], co-precipitation method [7], hydrothermal route [8], sol-gel [9], *etc*. However, in the conventional solid state synthesis, the oxides ceramics are obtained lengthy heat treatments and provide strong agglomeration effects with large grain size and inhomogeneous grain growth during sintering process [10]. Thus, sol-gel technique has more advantages than solid state method to obtained ultrafine nano sized powders with precise stoichiometry and better uniform size. Besides, sol-gel method has the advantage of lower processing temperatures, short annealing times, high purity of materials, good control of size and shape of the particles and particle size well below 100 nm at the lower processing temperature [11]. In this work, we reported the effect of sintering temperature on structure, microstructure and magnetic properties of single phase $La_{0.67}Ca_{0.33}MnO_3$ were synthesized using sol-gel reaction method.

EXPERIMENTAL

$La_{0.67}Ca_{0.33}MnO_3$ (LCMO) compound were prepared via sol-gel method by dissolving a stoichiometric mixture of nitrates cation ($La(NO_3)_3.6H_2O$, $Ca(NO_3)_2.4H_2O$ and $Mn(NO_3)_2.4H_2O$) in distilled water. Stoichiometric amount of the nitrate solution was stirred and heated at 70°C for 2hrs. Then, the aqueous solution of citric acid was added to the cationic mixture and after a while the ethelene glycol was added to the mixed solution. Finally, the whole solution was heated at 80°C with 250 rpm using magnetic stirrer until the gel is formed. On further heating, the gel was dried in the oven at 120°C until the gel was decomposed and produced a fluffy dried mass. The fluffy dried mass was ground and calcined at 500°C in ambient atmosphere for 5 hours with the heating and cooling rate of 2°C/min. Then, this powders were sintered with various temperature starting from 600°C to 1200ºC labeled as LC-SG6, LC-SG7, LC-SG8, LC-SG9, LC-SG10, LC-SG11 and LC-SG12, respectively. The structural and microstructure of the samples were characterized by X-ray diffraction (XRD, Phillips PW 3040/60 Xpert Pro) using a CuKα radiation at room temperature and field emission scanning electron microscopy (FESEM, LEO1455 VSPEM, with an OXFORD INCA ENERGY 300EDX).The magnetic behaviors were measured by vibrating sample magnetometer (VSM, LakeShore 7440) at room temperature. Thermal analysis of LCMO sample was

measured by Thermogravimetric Analysis (TGA).

RESULTS AND DISCUSSIONS

Figure 1 shows TGA measurement of sol-gel precursor performed at heating rates of 2°C/min. The decomposition is observed in three stages of weight loss. The first weight loss between 53.87 to 135.57ºC is suspected as the evaporation of water and remained organic material, such as: ethylene glycol or nitrate. Second rapid mass loss observed between 135.57 to 387.76ºC is suspected as the degradation of polymer chain bond of sol-gel sample. However, a minor decomposition is observed between 388.78 to 548.50ºC, which is suggested to be related to the initial formation of LCMO phase. No significant huge weight loss can be found above 549ºC. This indicates no further significant chemical reaction above this temperature range. Hence, to investigate phase formation of LCMO, green powder was calcined at 500ºC followed by sintering temperature ranging from 600ºC to 1200ºC.

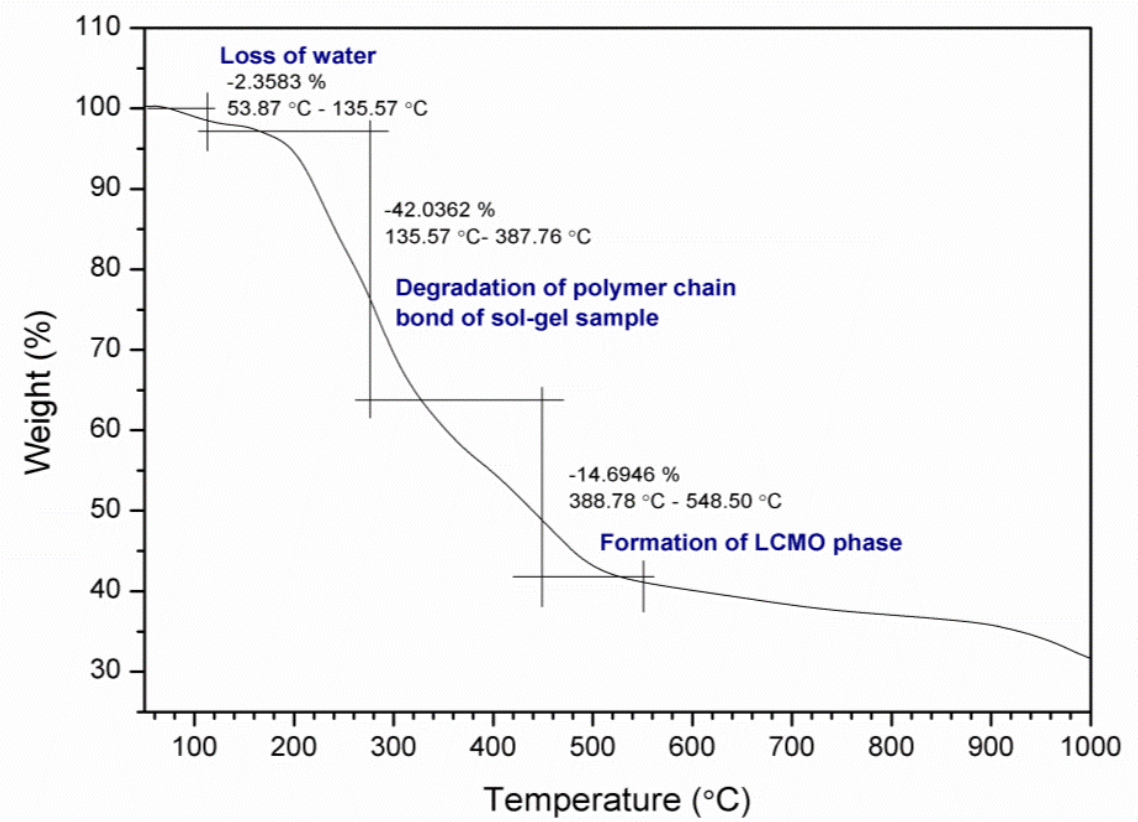

Figure 1: The Thermogravimetric analysis (TGA) for LCMO samples prepared via sol-gel method

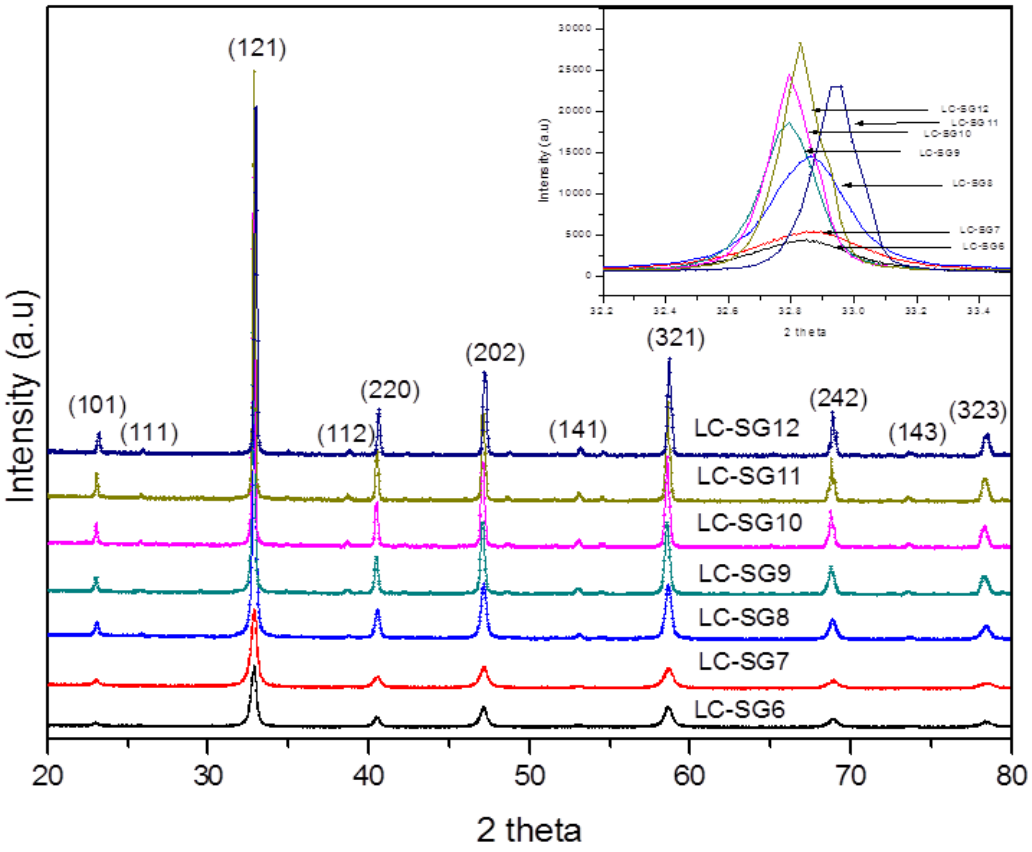

Figure 2: XRD patterns for LCMO with different sintering temperature from 600°C to 1200°C. [Inset] Peak of (121)

Figure 2 shows the XRD spectrums of LCMO with different sintering temperature from 600°C to 1200°C via sol-gel method. All synthesized samples are completely formed into polycrystalline single phase without any detectable impurities with orthorhombic structure having *Pnma* space group (62) (ICSD collection code: 82820). Inset figure 2 shows the (121) main peaks for all samples. The size of the crystallite was determined from the most intense of (121) peak. Using Scherrer's formula [12] and with $\lambda = 1.54$ Å, the crystallite size was calculated. The intensity of the X-ray peaks for the LCMO perovskite phase increases as sintering temperature increases from 600ºC to 1200ºC reflecting the growth of crystalline phase in all samples.

Table 1: Lattice parameter and Rietveld refinement data of all LCMO samples

Sample code	**LC-SG6**	**LC-SG7**	**LC-SG8**	**LC-SG9**	**LC-SG10**	**LC-SG11**	**LC-SG12**
ICSD Code	82820						
Structure	orthorhombic						
Space group	P n m a (62)						
***a* /Å**	5.4390(3)	5.4407(3)	5.4485(4)	5.4519(2)	5.4540(2)	5.4548(2)	5.4567(1)
***b* /Å**	7.6799(4)	7.6825(4)	7.6958(5)	7.7060(3)	7.7091(2)	7.7096(2)	7.7118(2)
***c* /Å**	5.4797(3)	5.4748(3)	5.4738(4)	5.4713(2)	5.4712(2)	5.4712(1)	5.4729(1)
Density g/cm^3	6.0633	6.0636	6.0455	6.0366	6.0319	6.0305	6.0249
Volume /Å^3	228.8449	228.8367	229.5202	229.8605	230.0373	230.0918	230.3048
∠Mn-O(1)-Mn (°)	160.533	160.207	160.195	160.181	160.179	160.179	160.179
∠Mn-O(2)-Mn(°)	161.931	160.783	160.818	160.850	160.859	160.860	160.860
Mn-O(1) (Å)	1.959	1.958	1.959	1.959	1.959	1.959	1.960
Mn-O(2) (Å)	1.947	1.948	1.951	1.954	1.954	1.955	1.955
R_P (%)	5.11980	5.41276	4.24989	4.33196	4.45114	4.75559	4.24316
R_{WP} (%)	6.44443	6.81812	5.43356	5.52936	5.74503	6.25637	5.92030
R_{EXP} (%)	4.66611	5.18654	3.64234	3.84189	3.74110	3.71808	3.91532
Goodness of fit (S)	1.90747	1.72812	2.22540	2.07138	2.35823	2.83144	2.28640
Lattice strain (%)	0.615	0.538	0.387	0.272	0.228	0.216	0.216
Crystallite size (nm)	20.2	23.1	32.4	46.3	55.6	58.7	58.3

Table 1 shows Rietveld Refinement fit to XRD data taken for all LCMO samples. The lattice constants of orthorhombic cell parameters *a, b, c* and the unit cell volume V≡ *abc* are extracted from Rietveld Refinement. As sintering temperature increased from 600°C to 1200°C, no significant changed on its cell volume. However, the lattice strain of the LCMO samples is decreased and crystallite size increase as tabulated in the Table 1. The average crystallite size that has been calculated are 20.2, 23.1, 32.4, 46.3, 55.6, 58.7 and 58.3 nm for LC-SG6, LC-SG7, LC-SG8, LC-SG9, LC-SG10, LC-SG11, LC-SG12 respectively. Hence, sintering at higher temperature promote crystallite growth and release internal strain.

Figure 3 shows the FESEM micrograph of the internal section of $La_{0.67}Ca_{0.33}MnO_3$ at different sintering temperatures (T_s). We might expected that ceramics prepared by sol-gel method have better homogeneity phase as well as physical properties. The micrographs showed that increasing sintering temperatures (T_s) promotes grain growth. As sintering temperature increase, the calculated average grain size of LC-SG6, LC-SG7, LC-SG8, LC-SG9, LC-SG10, LC-SG11, LC-SG12 were 29.29, 37.20 nm, 62.46 nm, 127.92 nm, 256.43 nm, 432.56 nm, and 722.48 nm, respectively. LC-SG6 sample give grain size distribution between 20 nm- 35 nm with average grain size of 29.29 nm. This sample had smaller grain sizes and hence its connection area is small in which resulting poor electrical connectivity. For the highest sintering temperature LC-SG12, pore is located between groups of grains. This was consequences of conglomeration of smaller grains or strong diffusion of two or more grain to form a bigger grain, the grains become more densely packed resulting in narrowing of the effective grain boundary

regions. Since higher sintering temperatures are expected to yield larger crystallite sizes and re-crystalline activity, the lattice strain is expected to be smaller for small sized grains. This strain relaxation with increasing grain size can lead to a reduction in the orthorhombicity system and hence slightly increased the lattice parameters.

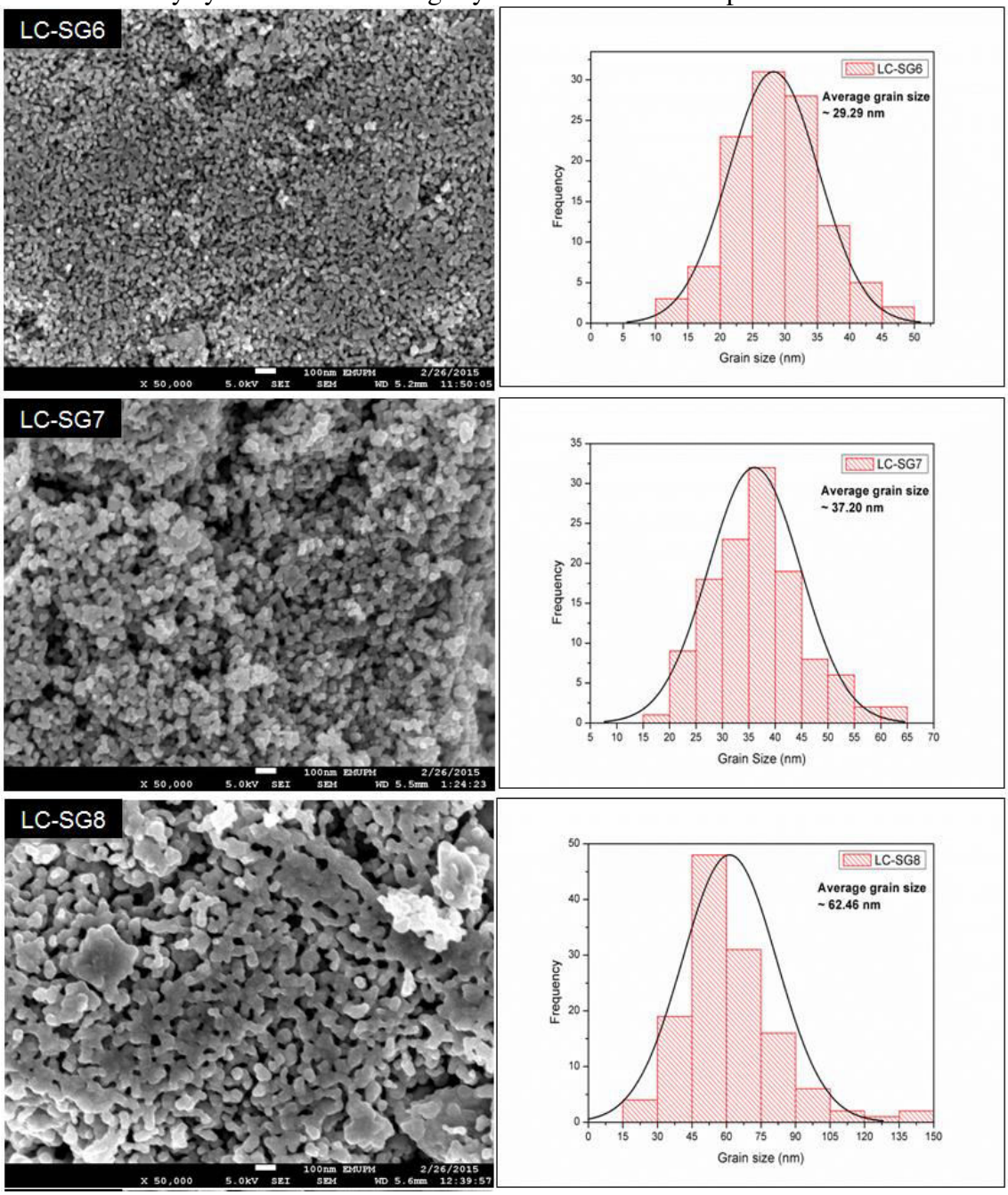

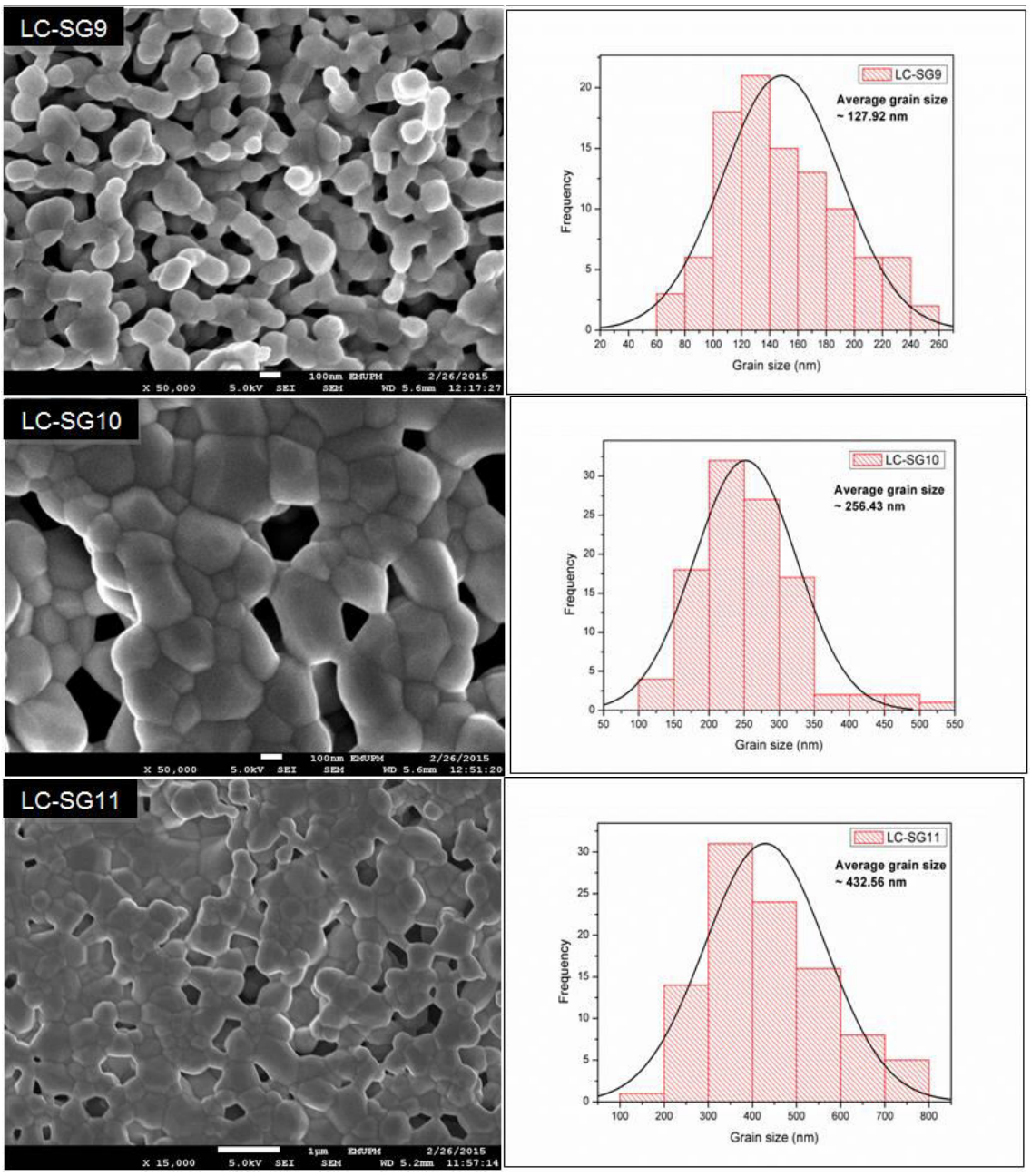
LC-SG9
X 50,000 5.0kV SEI SEM WD 5.6mm 12:17:27
LC-SG9
Average grain size
~ 127.92 nm
Frequency
Grain size (nm)
LC-SG10
X 50,000 5.0kV SEI SEM WD 5.6mm 12:51:20
LC-SG10
Average grain size
~ 256.43 nm
Frequency
Grain size (nm)
LC-SG11
X 15,000 5.0kV SEI SEM WD 5.2mm 11:57:14
LC-SG11
Average grain size
~ 432.56 nm
Frequency
Grain size (nm)

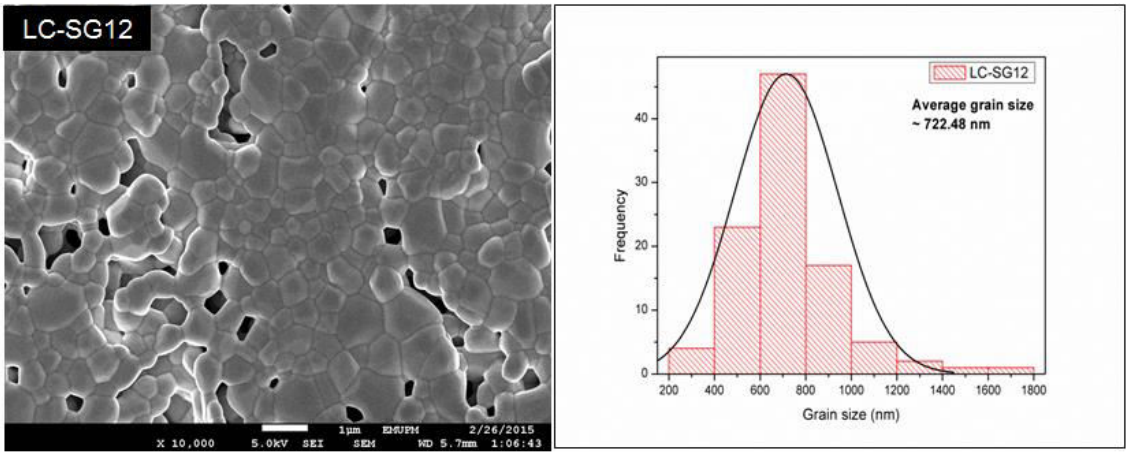

Figure 3: Field emission scanning electron micrograph (FESEM) with grain size distribution for all LCMO sample sintered from 600ºC to 1200°C

The variation of the crystallite sizes (CS) obtained from the FWHM of the X-ray diffractions peaks and the grain size (GS) obtained from FESEM micrograph for the all LCMO samples are tabulated in Table 2 and plotted in Figure 4. The growth rate of the crystallite size is slower as compared to grain size and reaches saturation above 1000ºC. The difference between CS and GS was more pronounced at higher sintering temperature. Both crystallite sizes (CS) and the grain size (GS) increases with sintering temperature (T_s) due to congregation of the grains because a grain may consist of several crystallite domains and these domains arises due to twinning and other structure defects such as vacancies, dislocations, stacking faults in the grain [13]. Generally, at low sintering temperature (600ºC and 700ºC) it is expected that only single crystallite on each grain and at higher temperature (1000ºC-1200ºC), the grain might consist of multi crystallite.

Table 2: Grain size (GS) and crystallite size (CS) dependence on the sintering temperature

Sample	Sintering Temperature, (T_s)/°C	Grain Size (GS)/ (nm)	Crystallite Size (CS)/ (nm)
LC-SG6	600	29.29	20.2
LC-SG7	700	37.20	23.1
LC-SG8	800	62.46	32.4
LC-SG9	900	127.92	46.3
LC-SG10	1000	256.43	55.6
LC-SG11	1100	432.56	58.7
LC-SG12	1200	722.48	58.3

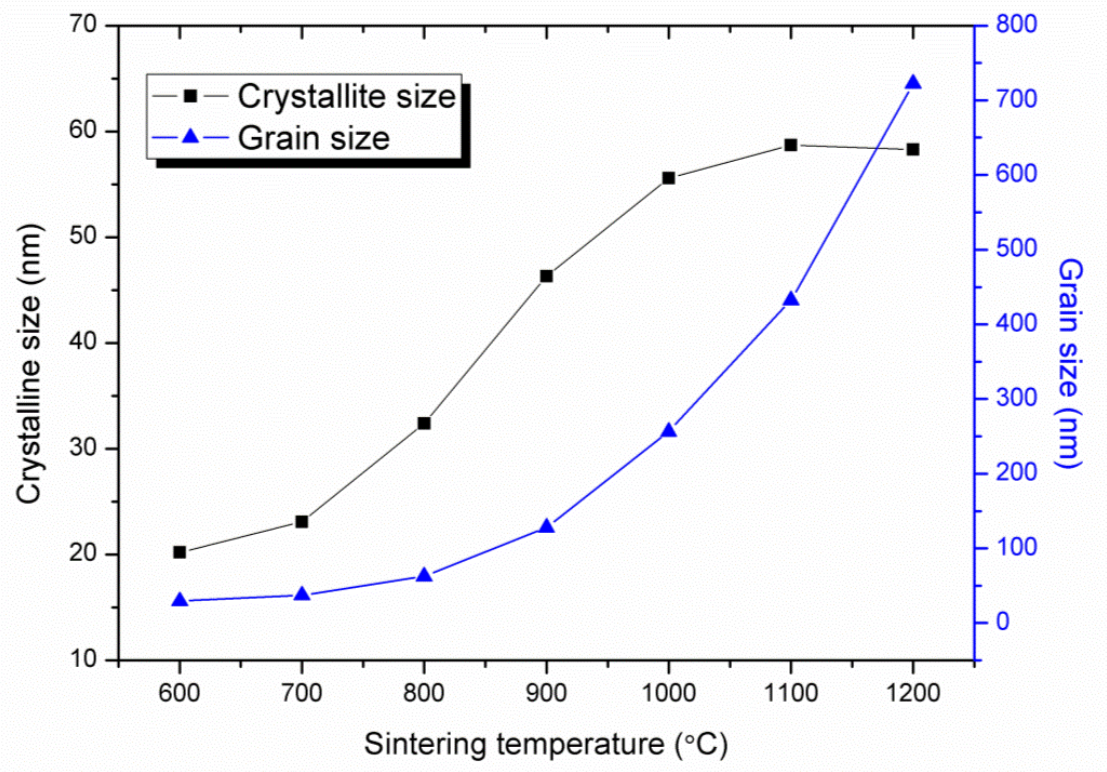

Figure 4: Crystalline size and grain size dependence on sintering temperature

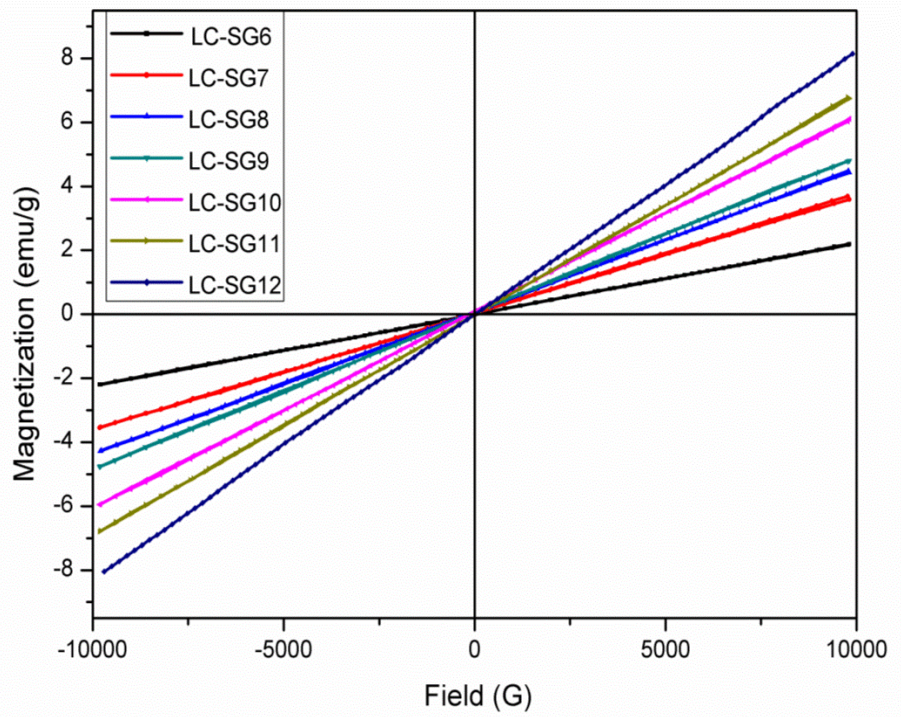

Figure 5: Magnetization versus magnetic field at room temperature for all LCMO sample

From Figure 5, all LCMO samples with different sintering temperature exhibit paramagnetic measured by Vibrating Sample Magnetometer (VSM) at room temperature. The magnetization of LCMO samples were increases with the grain size. This can be ascribed to relatively poor crystallization and larger effective grain boundary surface contribution in smaller particles. The grain boundary or surface act as a magnetic shielding layer to protect the magnetic ordering in the core region. Hence, magnetization reduced with grain size.

Table 3: Coercivity (H_c), magnetization (M_s), Retentivity (M_r) dependence on grain size (GS) of all LCMO samples

Sample	Grain size (GS)/ nm	Coercivity (H_c)/ G	Magnetization (M_s)/emu/g	Retentivity (M_r)/memu/g
LC-SG6	29.29	9.1	2.2	2.1
LC-SG7	37.20	8.1	3.6	2.4
LC-SG8	62.46	24.7	4.4	12.3
LC-SG9	127.92	3.3	4.8	1.7
LC-SG10	256.43	0.8	6.0	0.1
LC-SG11	432.56	2.2	6.7	4.0
LC-SG12	722.48	0.6	8.2	3.2

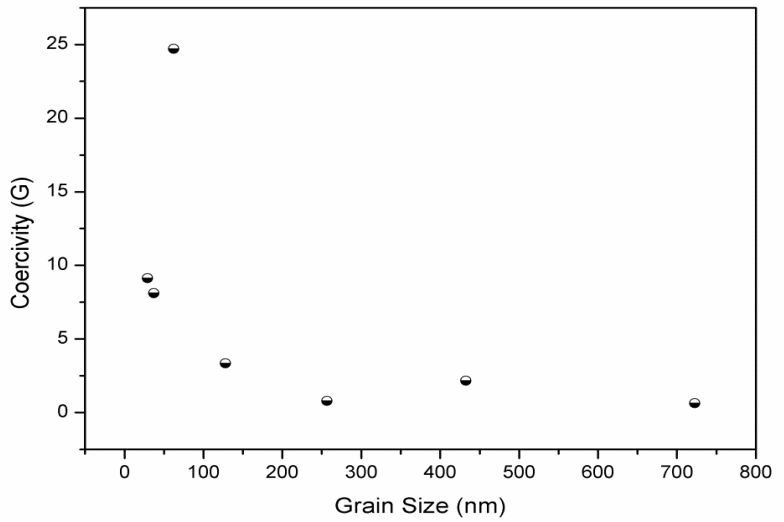

Figure 6: Grain size dependence of coercivity and remanence of LCMO sample

Table 3 displays coercivity (H_c), magnetization (M_s), retentivity (M_r) dependence on grain size (GS). The maximum coercivity of 24.7G is observed for LC-SG8 sample where others sample show lower coercivity. Refer to Table 2, we believed that transition of single domain (SD) to multi domain (MD) occurred as the grain size increased from 29.3nm to 722.5nm. LC-SG8 is believed in two domain or pseudo-single domain state. Two domains were tried to squeeze in one grain which resulting

thinner domain wall. Therefore, the magnetostatic and exchange energy is larger. Hence, energy that needed to rotate the whole magnetization of the grain of LC-SG8 sample is magnetically harder and had higher coercivity. For the smaller grain sizes of LC-SG6 and LC-SG7, coercivity decrease due to the randomizing effects of thermal energy meanwhile, for larger grain sizes of LC-SG9, LC-SG10, LC-SG11 and LC-SG12, the coercivity decreases as the grain subdivides into more domain, hence lower it magnetostatic energy.

CONCLUSION

We have demonstrated the effects of sintering temperature on microstructures and magnetic properties of nanoparticles of polycrystalline $La_{0.67}Ca_{0.33}MnO_3$ ceramics by sol-gel method. As T_s increase from 600°C to 1200°C, the grain size increased from 29 nm to 722 nm and crystallite size increased due to congregation effect. The rietveld refinement shows no significant change on the lattice parameter. Typical evolution from single-domain to multi-domain condition had been recorded as the grain size increase. The highest coercivity of 24.7 G had been obtained in LC-SG8 sample which is believed in two domain or pseudo-single domain condition that due to magnetostatic and exchange energy effect.

ACKNOWLEDGEMENTS

The authors gratefully acknowledge the support from the Ministry of Education (MOE) forthe grant under the Fundamental Research Grant Scheme (FRGS) vote: 02-01-14-1469FR: *Enhancement of Magnetoresistance Effect in La-(Sr, Ca)-Mn-O/Sb_2O_3, CeO_2, Al_2O_3 Composites for Low-Field Magnetic Sensor*.

REFERENCES

[1] J. Ma, M. Theingi, Q. Chen, W. Wang, X. Liu, and H. Zhang, *Ceram. Int.*, **39** 7839–7843 (2013)
[2] L. E. Hueso, F. Rivadulla, R. D. Sa, D. Caeiro, and C. Jardo, *J. Magn. Magn. Mater.*, **189** 321–328 (1998)
[3] G. Venkataiah, D. C. Krishna, M. Vithal, S. S. Rao, S. V. Bhat, V. Prasad, S. Subramanyam, and P. Reddy, *Phys. B Condens. Matter*, **357**, 370–379 (2005)
[4] U. K. Goutam, P. K. Siwach, H. K. Singh, R. S. Tiwari, and O.N.Srivastava, *J. Phys. D Appl. Physics,* **39** (1) 1–21 (2006)
[5] Y.-H. Huang, K.-F. Huang, F. Luo, L.-L. He, Z.-M. Wang, C.-S. Liao, and C.-H. Yan, *J. Solid State Chem.*, **174** (2) 257–263 (2003)
[6] G. Campillo, Gil, O. Arnache, J. J. Beltrán, J. Osorio, and G. Sierra, *J. Phys. Conf. Ser.*, **466** 012-022 (2013)
[7] Z. F. Zi, Y. P. Sun, X. B. Zhu, Z. R. Yang, J. M. Dai, and W. H. Song, *J. Magn. Magn. Mater.*, **321** (15) 2378–2381 (2009)
[8] W. L. Sin, K. H. Wong, and P. Li, *Acta Phys. Pol. A*, **111** (1) 165–171 (2007)
[9] D. Das, P. Chowdhury, R. N. Das, C. M. Srivastava, and A. K. Nigam, *J. Magn.*

Magn. Mater., **3** (2) 178–184, (2002)
[10] H. Shen and S. Mathur, *J. Sol-Gel Sci. Technol.*, **25** 147–157 (2002)
[11] J. Ma, M. Theingi, Q. Chen, W. Wang, X. Liu, and H. Zhang, *Ceram. Int.*, **39** 7839–7843 (2013)
[12] D. Das, a. Saha, S. E. Russek, R. Raj, and D. Bahadur, *J. Appl. Phys.*, **93** (10) 8301 (2003)
[13] P. K. Siwach, R. Prasad, A. Gaur, H. K. Singh, G. D. Varma, and O. N. Srivastava, *J. Alloys Compd.*, **443** 26–31 (2007)